

## SANS study of new magnetic nanocomposites embedded into the mesoporous silica

E.A. Kelberg<sup>a,\*</sup>, S.V. Grigoriev<sup>a,b</sup>, A.I. Okorokov<sup>a</sup>, H. Eckerlebe<sup>c</sup>,  
N.A. Grigorieva<sup>d</sup>, W.H. Kraan<sup>b</sup>, A.A. Eliseev<sup>e</sup>, A.V. Lukashin<sup>e</sup>,  
A.A. Vertegel<sup>e</sup>, K.S. Napolkskii<sup>e</sup>

<sup>a</sup> Petersburg Nuclear Physics Institute, Gatchina, St. Petersburg 188300, Russia

<sup>b</sup> Interfaçtaul Reactor Instituut, TU-Delft, 2629 JB Delft, The Netherlands

<sup>c</sup> GKSS Forschungszentrum, 21502 Geesthacht, Germany

<sup>d</sup> St. Petersburg State University, St. Petersburg 198504, Russia

<sup>e</sup> Higher School of Materials Science, Moscow State University, Moscow 119899, Russia

---

### Abstract

Magnetic nanocomposites embedded into mesoporous silica have been studied by Small Angle Polarized Neutron Scattering. It is well known that mesoporous silica represents a highly regular hexagonal structure of nanotubes. For the samples under study a diffraction peak in SANS at  $q_c \approx 1.7 \text{ nm}^{-1}$  is observed which corresponds to a hexagonal structure with periodicity  $a \approx 3.5 \text{ nm}$ . We found that the intercalation of iron into the silica matrix leads to some changes of the matrix itself. Additionally, the nuclear–magnetic interference in scattering of polarized neutrons was investigated. The interference reveals the absence of a periodical magnetic structure at room temperature which would be consistent with the hexagonal structure of nanotubes. The correlation between magnetic nanoparticles and pores of the matrix is revealed in the interference scattering at  $q \ll q_c$ .

© 2003 Published by Elsevier Science B.V.

**Keywords:** Mesoporous silica; Diffraction; SANS; Nuclear magnetic interference

---

### 1. Introduction

Nanomaterials have attracted much attention in recent years [1–3] because of their numerous applications in many branches of industry. There are several methods to synthesize nanoparticles. Probably, the most popular one is to synthesize in a confined-geometry system or synthesis in solid phase nanoreactors [4]. In this way, the nanopar-

ticles are protected both from external influences and aggregation is prevented. This method also provides a high monodispersity of the particles. Mesoporous silica  $\text{SiO}_2$  is commonly used as a matrix due to its homogenous, regular structure of pores and high chemical resistance [5]. The large-scale periodicity with a lattice constant of few nanometers makes this structure a suitable object for study by small angle neutron scattering. In SANS studies of such a structure one can observe a diffraction peak in the  $q$ -dependence. Then one may follow the changes in characteristics of the

---

\*Corresponding author.

E-mail address: [kelberg@pnpi.spb.ru](mailto:kelberg@pnpi.spb.ru) (E.A. Kelberg).

peak when iron is introduced into the porous structure. Additionally, we have used polarized neutrons to study the properties and the geometry of the magnetic subsystem.

## 2. The samples

Mesoporous silica is a promising matrix for the preparation of nanocomposites. One could expect that the size and the shape of the nanoparticles incorporated into the mesoporous silica would be consistent with the dimensions of the porous framework. Recently, several attempts have been made to prepare metal nanoparticles in mesoporous silica matrix by soaking mesoporous  $\text{SiO}_2$  in an aqueous solution of the corresponding metal salt followed by reduction of the metal caution [6]. However, it was found that the size of metal particles exceeds the size of the pores and the particle size distribution is not uniform. The reason for the formation of nanoparticles outside the pores is probably the hydrophobic nature of the pore walls [7], which prevents filling the pores by an aqueous solution. Another approach involves vapour deposition of a volatile metal compound into the pores with subsequent reduction [8,9]. This method was more successful resulting in the formation of Ge, Pd and Pt wires, whose diameter was consistent with the diameter of the pores. However, this method cannot be used for the preparation of magnetic nanowires since reduction of volatile compounds of magnetic metals (e.g., Fe, Co, Ni) occurs at relatively high temperature, which results in the collapse of nanowires [8]. Iron nanoparticles in the  $\text{SiO}_2$  matrix were then synthesized by reduction in hydrogen at temperatures  $T = 260^\circ\text{C}$ ,  $300^\circ\text{C}$ ,  $350^\circ\text{C}$ ,  $375^\circ\text{C}$  and  $400^\circ\text{C}$ . The samples obtained were denoted as  $\text{FeSiO}_2$ -260,  $\text{FeSiO}_2$ -300,  $\text{FeSiO}_2$ -350,  $\text{FeSiO}_2$ -375 and  $\text{FeSiO}_2$ -400, respectively. The suggested method results in the formation of iron nanowires inside the silica framework. The diameter of the nanowires is consistent with that of the pores. Finally, the powder consisting of small particles of mesoporous silica was used for the study. In the present work, we suggest a novel variant of the synthesis of ordered magnetic iron

nanowires in the mesoporous silica matrix. The method is based on the introduction of a hydrophobic metal compound,  $\text{Fe}(\text{CO})_5$ , into the hydrophobic part of the as-prepared mesoporous silica-surfactant composite.

## 3. Experimental

The SANS experiments were carried out at the SANS-2 scattering facility of the FRG-1 research reactor in Geesthacht (Germany). The beam of polarized neutrons with initial polarization  $P_0 = 0.9$ , wavelength  $\lambda = 0.58 \text{ nm}$  ( $\Delta\lambda/\lambda = 0.1$ ) and divergence of  $1.5 \text{ mrad}$  was used. The scattered neutrons were detected with a position sensitive detector with  $128 \times 128$  pixels. An external magnetic field of  $0.25 \text{ T}$  was applied in the horizontal plane and perpendicularly to the incident beam in order to reveal nuclear magnetic cross-correlator of the system [10,11].

For SANS, in general, the cross-section of polarized neutrons consists of nuclear and magnetic contributions, as well as a nuclear–magnetic interference contribution of the scattering:

$$\frac{d\sigma}{d\Omega} = |A_n|^2 \mathcal{F}_n(\vec{q}) + |A_m|^2 m_\perp^2 \mathcal{F}_m(\vec{q}) + 2\vec{P}_0 \vec{m}_\perp (A_n A_m \text{Re} \mathcal{F}_{nm}(\vec{q})), \quad (1)$$

where  $A_n = (bN_0)$  is the nuclear contrast (with  $b \simeq 0.4 \times 10^{-12} \text{ cm}$  as the average nuclear scattering length,  $N_0$  as average atom density) and where  $A_m = rN_0$  (with  $r = 0.54 \times 10^{-12} \text{ cm}$ ) is the magnetic contrast.  $\vec{m}$  is the unit vector along the magnetization and  $m_\perp = \vec{m} - (\vec{m} \cdot \vec{e}) \vec{e}$  with  $\vec{e} = \vec{q}/q \mathcal{F}_{n(m)}(\vec{q}) = |F_{n(m)}|^2$  is the autocorrelation function of the nuclear (magnetic) density with  $F_{n(m)}(q)$  as a Fourier image of the form-factor of the particle. The cross correlator of the nuclear–magnetic density fluctuations is given by:  $\mathcal{F}_{nm}(\vec{q}) = \overline{F_n^*(q) F_m(q)}$ . The magnetic nanoparticles in our case are expected to be superparamagnetic and therefore the magnetic scattering is small as compared with the nuclear one. Fortunately, the interference scattering depends linearly on the magnetic scattering amplitude and therefore it has to be much larger than the pure magnetic contribution.

We determine the total (nuclear and magnetic) scattering as:  $I(q) = I^+(q) + I^-(q)$ . The polarization-dependent part of the scattering is determined as the difference  $\Delta I(q) = I^+(q) - I^-(q)$  of the intensities for neutrons polarized parallel (+) and anti-parallel (−) to the magnetic field.

#### 4. Results

A typical example of a three-dimensional picture of neutron scattering in the sample  $\text{FeSiO}_2\text{-375}$  is presented in Fig. 1. If neutrons are scattered by the regular two-dimensional structure of nanotubes of a single particle then they form two spots of intensity at  $q = \pm 2\pi/a$ , where  $a$  is the lattice constant. This relation corresponds to the Bragg condition. The spots are located in the directions perpendicular to the long direction of the nanotubes. Since the particles in a powder are randomly oriented, the spots from different particles form a ring of scattered intensity at certain constant  $|q|$ . In order to obtain better statistics, we average the intensity over  $2\pi$  at constant  $|q|$ .

The  $q$ -dependence of the neutron intensity  $I(q)$  for a pure  $\text{SiO}_2$  matrix and the sample  $\text{FeSiO}_2\text{-375}$  is shown in Fig. 2. The data were fitted with the expression  $I(q) = A_1/q^4 + A_2\omega^2/((q - q_c)^2 + \omega^2)$ .

The first term describes scattering from the particles and their surfaces while the second term describes the diffraction peak centered at  $q_c$  with a width of  $\omega$ . It was found that the intercalation of iron into the matrix leads to a shift of  $q_c$  toward smaller  $q$ . Thus for the pure matrix  $q_c = 1.74 \pm 0.01$  and for  $\text{FeSiO}_2\text{-375}$   $q_c = 1.70 \pm 0.01$ . Therefore, the lattice parameter  $a$  increases. We interpret this fact as if the iron fills the pores and pushes neighbouring tubes apart, thus making the constant  $a$  bigger. Additionally, the intensity at small  $q < 1 \text{ nm}^{-1}$  increases for the samples with iron. This implies the formation of clusters and possibly a partial destruction of the porous structure during synthesis of  $\text{FeSiO}_2$  nanocomposites.

To clarify the question of the location of the intercalated iron inside the matrix, we used polarized neutrons. On the basis of the regular porous structure, it was expected that nuclear-magnetic interference scattering would be observed if a network of iron magnetic nanowires appears. However, interference scattering was observed in the small  $q$ -range but not at the peak position. Fig. 3 shows the value of the polarization  $P = \Delta I/I$  as a function of  $q$ . The polarization has a maximum at  $q \approx 0.3 \text{ nm}^{-1}$ . The interference correlation length may be estimated as

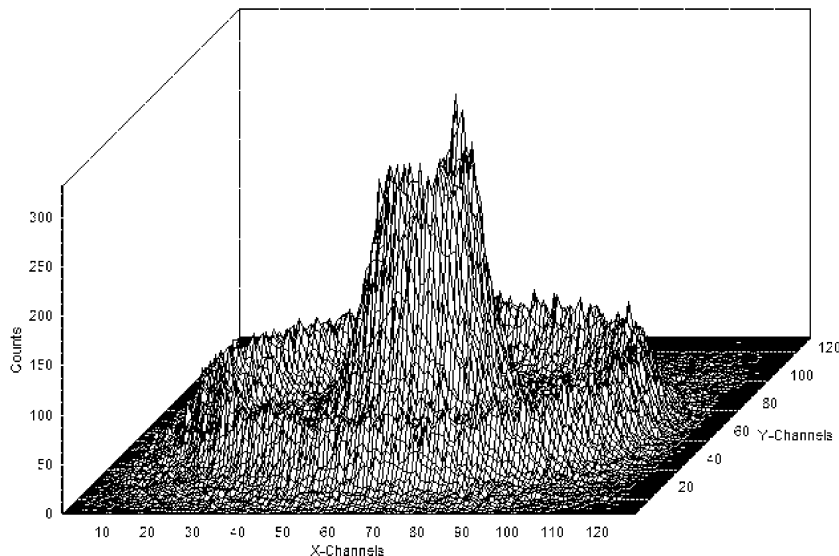


Fig. 1. Typical three-dimensional pattern of the small angle scattering from mesoporous silica with embedded iron nanoparticles.

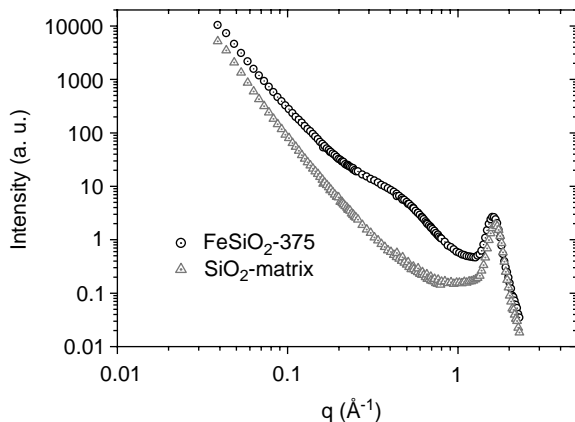


Fig. 2.  $q$ -dependence of the scattering intensity for pure mesoporous silica  $\text{SiO}_2$  and for the sample  $\text{FeSiO}_2$ -375 at  $H = 0.25$  T.

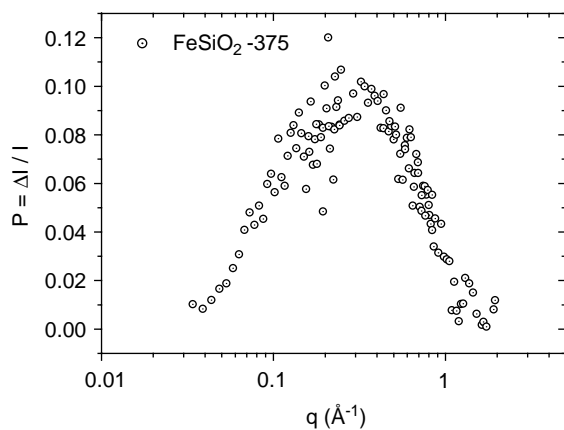


Fig. 3.  $q$ -dependence of the polarization  $P = \Delta I/I$  for the sample  $\text{FeSiO}_2$ -375 at  $H = 0.25$  T.

$R_{\text{int}} \approx 2\pi/q = 20$  nm. The absence of interference at the diffraction peak position with a simultaneous presence of interference in the range of small  $q$  may be interpreted in the following way. The iron nanowires consist of the partially crystalline and partially amorphous pieces which are randomly distributed along the wires. The crystalline pieces are ferromagnetic ones with high density. The amorphous iron pieces are superparamagnetic

with low density. Thus, they form the nuclear magnetic correlated network that provides the appearance of the interference in the scattering. Further experiments are planned to study the magnetic properties of the system of magnetic nanowires in a wide range of temperature and magnetic field.

### Acknowledgements

The authors like to thank for partial support RFFR (projects 00-15-96814, 00-15-97435 and 01-02-17286), INTAS 2001-03-204 and the Russian State Program “Neutron Research of Solids”. The PNPI-team acknowledges GKSS—Geesthacht for hospitality.

### References

- [1] E. Prouzet, F. Cot, G. Nabias, A. Larbot, P. Kooyman, T.J. Pinnavaia, *Chem. Mater.* 11 (1999) 149.
- [2] Q. Huo, D.I. Margolese, G.D. Stucky, *Chem. Mater.* 8 (1996) 1147.
- [3] L. Bronstein, E. Kramer, B. Berton, C. Burger, S. Forster, M. Antonietti, *Chem. Mater.* 11 (1999) 1402.
- [4] J.H. Fendler, *Chem. Mater.* 8 (1996) 1616.
- [5] J.S. Beck, J.C. Vartuli, W.J. Roth, M.E. Leonovicz, C.T. Kresge, K.D. Shmitt, C.T.-W. Chu, D.H. Olson, E.W. Sheppard, S.B. McCullen, J.B. Higgins, J.L. Schlenker, *J. Am. Chem. Soc.* 114 (1992) 10834.
- [6] J.S. Beck, J.C. Vartuli, W.J. Roth, M.E. Leonovicz, C.T. Kresge, K.D. Shmitt, C.T.-W. Chu, D.H. Olson, E.W. Sheppard, S.B. McCullen, J.B. Higgins, J.L. Schlenker, *J. Am. Chem. Soc.* 114 (1992) 10834.
- [7] G. De, L. Tapfer, M. Catalano, G. Battaglin, F. Caccavale, F. Gonella, P. Mazzoldi, R.F. Haglung, *Appl. Phys. Lett.* 68 (26) (1996) 3820.
- [8] C. Jinwoo, K. Lee, H. Kang, S.J. Oh, H.-C. Ri, *Mater. Res. Soc. Symp.* 635 (2001) 3.3.1.
- [9] M.J. MacLachan, P. Aroca, N. Coombs, I. Manners, G.A. Ozin, *Adv. Mater.* 10 (1998) 144.
- [10] A. Wiedenmann, *Physica B* 297 (2001) 226.
- [11] V.V. Runov, G.P. Kopitsa, A.I. Okorokov, M.K. Runova, H. Glattli, *JETP Lett.* 69 (4) (1999) 353.